  DOI 10.1515/htmp-2012-0030

The Effects of the Withdrawal Rate and Heat Treatment on the Microstructure of Directionally Solidified Nb-14Si-24Ti Alloy

Ligang Wang,[1] Fei Ding,[1] Sainan Yuan,[1] Lina Jia[1] and Hu Zhang[1,*]

[1] Department of Materials Science and Engineering, Beijhang University, Beijing, China

Abstract. In this work, an Nb-14Si-24Ti alloy (at.%) was prepared by liquid-metal-cooled directional solidification (DS) and then heat treated (HT) at 1450°C for 100 h. The effects of the withdrawal rate and heat treatment on the microstructure were investigated. The results show that the DS samples consisted of Nb_{SS} dendrites, Nb_3Si blocks and eutectic Nb_{SS}/Nb_3Si. As the withdrawal rate increased, the microstructure became finer, the volume fraction of eutectic Nb_{SS}/Nb_3Si increased and the morphology of eutectic cell transformed from petaloid to regularly arranged granular morphology. The microstructure of the HT samples consisted of Nb_{SS} and Nb_3Si. The metastable phase of Nb_3Si did not discompose through the eutectoid reaction. The dendritic Nb_{SS}connected through diffraction and the secondary dendrite arm got coarser. The boundary of eutectic Nb_{SS}/Nb_3Si became blurry and the black Ti-rich phase of the DS samples in this region disappeared. The Nb_3Si connected to form the continuous matrix. The granular Nb_{SS} of eutectics spheroidized and the lamellar Nb_{SS} of eutectic interconnected and became more bending distributed uniformly in the Nb_3Si matrix.

Keywords. Nb-Si, directional solidification, heat treatment, microstructure.

PACS®(2010). 81.05.Bx.

1 Introduction

Nb-Si-based ultra-high-temperature alloys possess higher melting points (>1750°C), relatively lower densities (6.6–7.2 g/cm^3) and attractive high-temperature strength and oxidation resistance properties [1–5]. Therefore, Nb-Si-based alloys show great promise for application as the next generation turbine airfoil materials at the temperature of up to 1300°C.

In Nb-Si-based alloys, the solid solution (Nb_{SS}) supplied the room-temperature toughness, the intermetallic phases were of benefit to the high-temperature strength. Recent researches have focused on alloying and processing technologies for enhancing the combined properties [4, 6, 7]. A range of processes, including vacuum non-consumable tungsten electrode arc-melting, powder metallurgy processing and directional solidification, was used to produce Nb-Si-based alloys [7–12]. The directional solidification technique could result in Nb-Si-based alloys with a desired morphology of the solid solutions and intermetallic phases distributed uniformly and aligned along the growth direction, which can also eliminate horizontal grain boundaries and enhance the longitudinal mechanical properties.

After more than ten years of research, multicomponent alloy system based on Nb-Si-Ti alloy system has been developed [5, 13–16] such as the Nb-Si-Ti-Cr-Al-Hf alloy from GE [17]. The alloy obtained a better balance of room-temperature toughness, high-temperature strength and oxidation resistance However, the room-temperature toughness was still too low to meet the operation requirement. How to optimize and control the alloy structure to obtain the higher room-temperature toughness have become a problem worthy of study. And the directional solidification and heat treatment are effective ways to optimize and control the alloy structure. However, the interactions between the alloying elements in multi-component alloys complicated the solidification progress.

To eliminate the effects of interactions between the alloying elements to the directionally solidification progress, in this work, an Nb-14Si-24Ti alloy was designed to explore the directional solidification path. A series of solidification parameters contributed to exploring the solidification characteristics and the effect of solidification condition on the phase composition and fracture toughness. The effects of the withdrawal rate and heat treatment on the microstructure were evaluated.

2 Experimental Procedures

With a nominal composition of Nb-14Si-24Ti (at.%), master alloy buttons were prepared by vacuum non-consumable arc-melting for four times to ensure homogeneity. Liquid metal-cooled directional solidification [18] was used

* **Corresponding author:** Hu Zhang, Department of Materials Science and Engineering, Beijhang University, Beijing, 100191, China; E-mail: zhanghu@buaa.edu.cn.

Received: March 10, 2012. Accepted: March 25, 2012.

in this study. Master alloy rods with a diameter of approximately 14 mm were prepared by electro-discharge machining (EDM). After grinding, ultrasonic cleaning and drying,the rods were assembled on the withdrawing device.Once a vacuum pressure of 1.0×10^{-3} Pa was reached, the furnace chamber was heated. When the temperature reached 1000°C, high purity (99.99 wt.%) argon was backfilled into the furnace chamber. After holding for 20 min at 1900°C, the samples were withdrawn at 1.2 mm/min, 6 mm/min and 18 mm/min. The withdrawal distance was set to 160 mm. The directionally solidified specimens with variable withdrawal rates were marked as DS1.2, DS6 and DS18. The specimens were cut open longitudinally from the middle.Half of the specimens were then heat treated (HT) at 1450°C for 100 h in a high vacuum heat treatment furnace. The samples were cooled in the furnace at a cooling rate of approximately 10°C/min. The heat-treated samples were marked as HT-1.2, HT-6 and HT-18.The longitudinal sections (parallel to the growth direction) in the DS regions of all specimens, ranging from 120 to 135 mm distance from the bottom, were collected as the regions of interest. The regions of interest on transverse sections focused at the position of 120 mm distance from the bottom.

Microstructural analysis was performed in a scanning electron microscope (SEM, QUANTA600) equipped with an energy dispersive X-ray spectroscopy (EDS, INCAPentaFETx3). The phases in cross-section of the DS specimen were identified by micro-area X-ray diffraction (XRD,D/max2200pc, Cu Ka) and the quantitative analysis was performed by Image-Pro Plus6.0.

3 Results and Discussion

3.1 The Microstructure of the Directionally Solidified (DS) Samples

Figure 1 shows the microstructure of typical growth morphologies of a directionally solidified alloy for different withdrawal rates at a constant temperature of 1900°C. According to the XRD and EDS results, the microstructure of the DS samples consisted of white dendritic Nb_{SS}, gray lath-like Nb_3Si, eutectic Nb_{SS}/Nb_3Si and Ti-rich regions distributed between the lath-like Nb3Si. From Figures 1 (a), (b) and (c), it can be seen that the dendrite structures were arranged mainly parallel to the axis in DS samples. As shown in Figures 1 (d), (e) and (f), the cross section morphology of the faceted Nb_3Si was mostly hexagonal. The secondary dendrite arms of Nb_{SS} were fully developed and the ternary dendrite arms were even observed in the DS sample withdrawn at 18 mm/min. Moreover, the eutectic Nb_{SS}/Nb_3Si, which presented petaline or regularly arranged granular morphology, was mainly distributed between the lath-like Nb_3Si.

The microstructure was sensitive to the withdrawal rate. With increasing withdrawal rate, the dendritic Nb_{SS} and lath-like Nb_3Si were both refined, and the primary dendrite arm spacing was also reduced obviously. The width of the primary dendrite arms of Nb_{SS} decreased from 30 μm to 5 μm, the width of the lath-like Nb_3Si decreased from 300 μm to 150 μm and the primary dendrite arm spacing decreased from 600 μm to less than 200 μm. Moreover, the deviations from the axis appeared smaller with increasing withdrawal rate, and the dendritic Nb_{SS} and lath-like Nb_3Si strictly grew along axis in the DS sample withdrawn at 18 mm/min.

With increasing withdrawal rate, the eutectic Nb_{SS}/Nb_3Si structure also changed obviously. As shown in Figures 1 (d) and (e), the Nb_{SS} grew perpendicular to the edge of eutectic cells, which made the eutectic structure presents radiated petaline morphology. As the withdrawal rate increased from 1.2 mm/min to 6 mm/min, the lamellar Nb_{SS} in petaline eutectic structure varied from curve to straight. When the withdrawal rate increased to 18 mm/min, the eutectic Nb_{SS} changed from lamellar to granular mostly and the lamellar Nb_{SS} was hardly observed in both longitudinal and transversal sections. With increasing withdrawal rate, it can be seen that the width of eutectic cells, the lamellar spacing and thickness of eutectic Nb_{SS} reduced obviously, whereas the volume fraction of eutectic increased. Moreover, in DS samples withdrawn at 1.2 mm/min and 6 mm/min, Nb_{SS}/Nb_3Si eutectic cells were distributed at only one end of the most lath-like Nb_3Si in the longitudinal sections . However, as shown in Figure 1 (f), in DS samples withdrawn at 18 mm/min these eutectic cells were distributed at each end of the lath-like Nb_3Si, in which the nuclei were Nb_3Si.

In the Ti-rich regions between the lath-like Nb_3Si (Figure 2) of the DS sample withdrawn at 1.2 mm/min, some lamellar Nb_{SS}/Nb_3Si structures were observed. According to the EDS results (Figure 2), the light phase was identified as $(Nb, Ti)_{SS}$ and the black one represented $(Nb, Ti)_5Si_3$. The average chemical composition of this lamellar region was near to that of $(Nb, Ti)_3Si$, so it can be deduced that lamellar Nb_{SS}/Nb_5Si_3 structures may form from the Nb_3Si through eutectoid reaction $Nb_3Si \longrightarrow Nb_{SS} + Nb_5Si_3$. However, only some Ti_{SS} and Ti-rich silicide were observed in the Ti-rich region in the DS samples withdrawn at 6 mm/min and 18 mm/min.

Figure 3 shows the microstructure of the longitudinal section in the DS sample withdrawn at 18 mm/min and the line scanning curves of Ti, Nb and Si elements.

As shown in Figure 3 (a), the center of the dendritic Nb_{SS} presented light white contrast, but the contrasts of the edge of the dendritic Nb_{SS} and the interdendritic region became dark. From Figure 3 (b), it can be seen that the interdendritic segregation was obviously, and there was more Ti contents at the edge of the dendritic Nb_{SS} and the interdendritic region than the center of the dendritic Nb_{SS}.

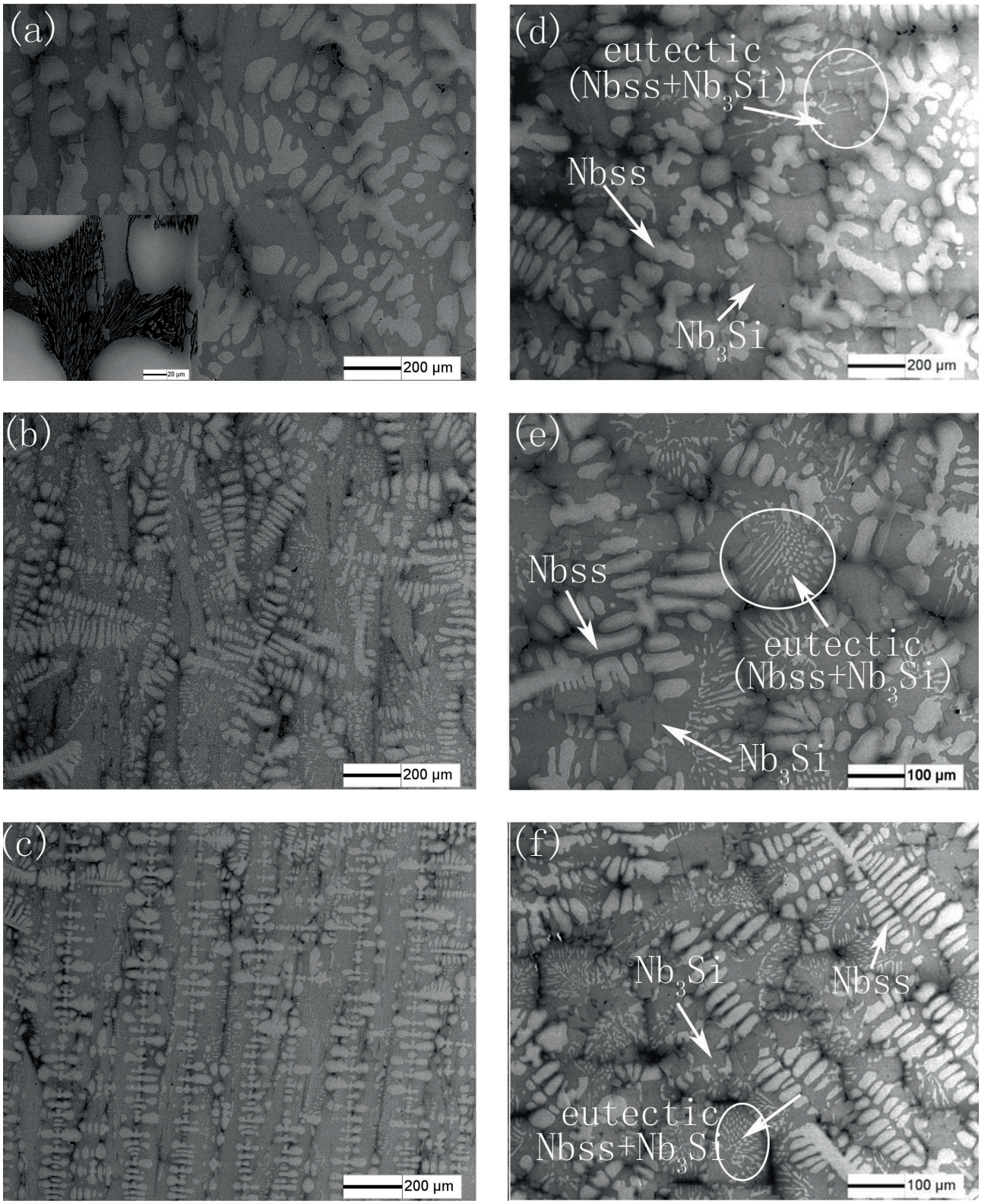

Figure 1. Longitudinal (a, b, c) and transverse (d, e, f) microstructures of a directionally solidified alloy for different withdrawal rates at a constant temperature rate of 1900°C: (a, d) 1.2 mm/min; (b, e) 6 mm/min; (c, f) 18 mm/min.

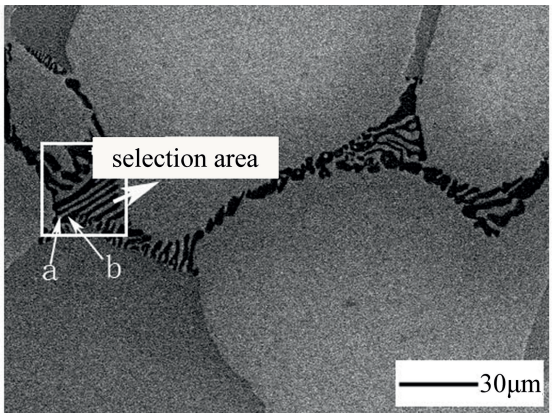

Phase	Composition, atomic(%)		
	Nb	Ti	Si
Light phase(a)	43.40	50.20	6.50
Dark phase(b)	27.91	37.97	34.12
Selection area	38.53	41.21	20 27

Figure 2. The microstructure of the eutectoid on transverse section of the DS sample withdrawn at 1.2 mm/min and the EDS results.

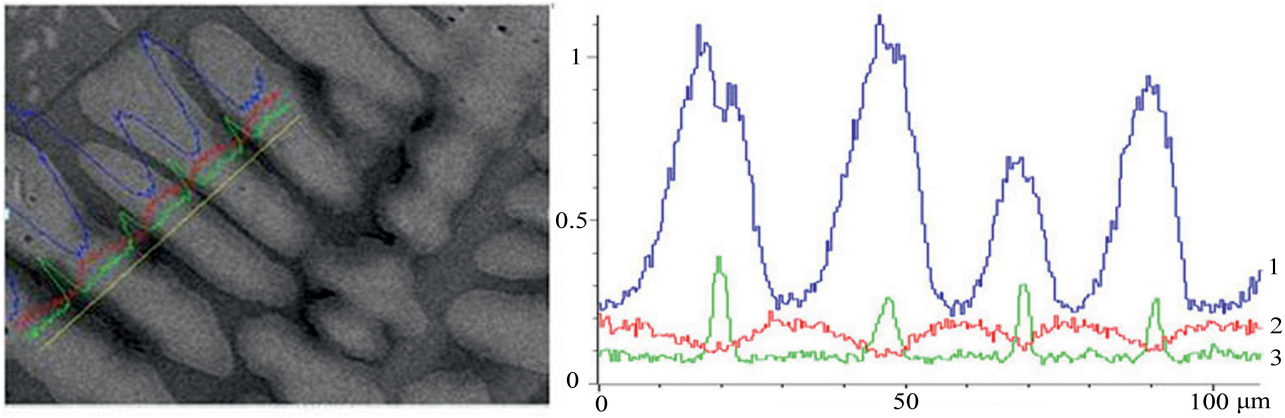

Figure 3. A backscattered electron image of the longitudinal section of the DS sample withdrawn at 18 mm/min and the line scanning curves of Ti (1), Nb (2) and Si (3).

3.2 Microstructures of the Heat-treated (HT) Samples

Figure 4 shows the microstructures of the heat-treated alloy. According to the XRD and EDS results, the phase composition in HT samples did not change with withdrawal rate. The white phase was Nb_{SS} and the gray phase was Nb_3Si. After heat treatment, the Nb_{SS} dendrites became continuous and the secondary dendrite arm became coarser. Meanwhile, the edges of Nb_{SS}/Nb_3Si eutectic cells became smooth. Additionally, the dark Ti-rich area disappeared gradually. The Nb_3Si blocks tended to became the matrix in the HT18 sample. In eutectic Nb_{SS}/Nb_3Si cells, the granular Nb_{SS} spheroidized after heat treatment, whereas the lamellar Nb_{SS} became more curved and interconnected, which was uniformly distributed in the Nb_3Si matrix.

Table 1 shows the EDS results of the Nb_3Si phases in DS and HT specimens. Compared to the DS samples, the Ti content increased in the HT specimens. This is because Ti element in the Ti-rich area diffused to Nb_3Si gradually during the heat treatment, and the Ti-rich area disappeared and the Nb_3Si phase became a matrix gradually. It can be seen from the comparison between Figure 4 (a) and Figure 4 (b) that a few Ti-rich regions remained between Nb_3Si blocks in the HT1.2 sample, whereas most of Nb_3Si blocks connected to be the matrix in the DS18 sample. It reveals that the element Ti diffused in the HT18 specimen more sufficiently. Hence, the Ti content in the HT18 sample was higher than that in the HT1.2 sample.

Alloy State	Phase	Composition, atomic fraction (%)		
		Nb	Ti	Si
DS1.2	$(Nb, Ti)_3Si$	57.17	19.69	23.13
HT1.2	$(Nb, Ti)_3Si$	55.54	21.41	23.05
DS18	$(Nb, Ti)_3Si$	57.73	18.16	24.11
HT18	$(Nb, Ti)_3Si$	59.98	23.44	26.58

Table 1. Compositions of the Nb3Si phases in DS and HT samples determined by EDS (at.%).

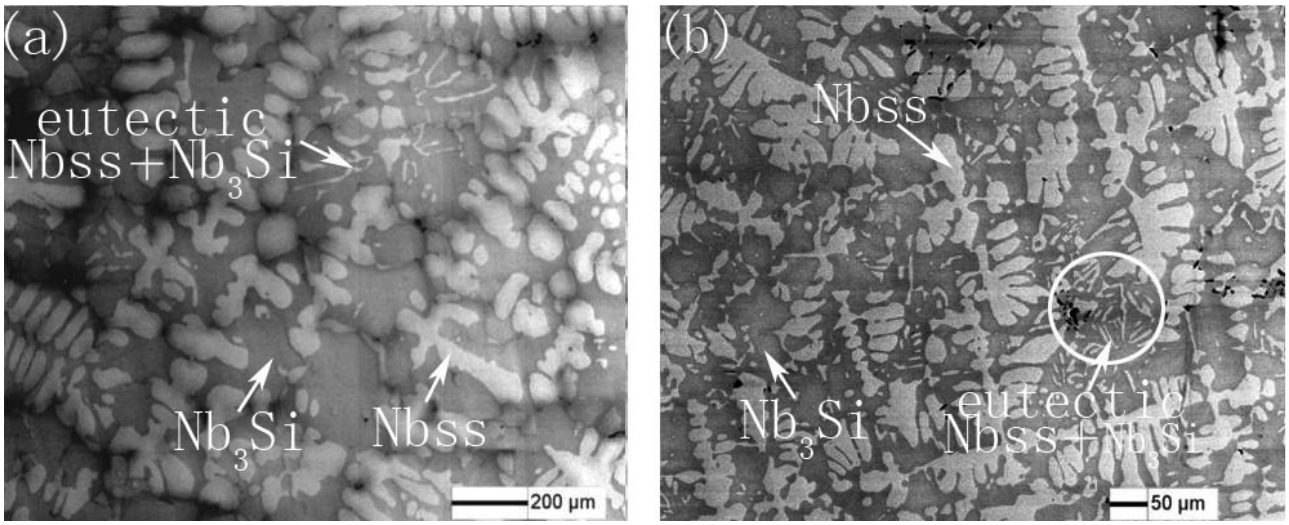

Figure 4. Microstructures of HT samples: (a) HT1.2; (b) HT18.

4 Conclusions

1) The DS specimens of the Nb-14Si-24Ti alloy consisted of Nb_{SS} dendrites, Nb_3Si laths and eutectic Nb_{SS}/Nb_3Si cells. Both the Nb_{SS} dendrites and the Nb_3Si laths were aligned erectly along the growth direction. The morphologies of eutectic Nb_{SS} were lamellar or regularly arranged granular.

2) The withdrawal rate had an important effect on the microstructure of the DS samples. With increasing withdrawal rate, both the Nb_{SS} dendrites and the Nb_5Si_3 became finer, and the volume fraction of eutectic cells increased. Additionally, the deviations from the axis appeared smaller with increasing withdrawal rate. The morphology of eutectic transformed from petaloid to regularly arranged granular morphology.

3) After heat treatment at 1450 °C for 100 hours, the HT specimens consisted of Nb_{SS} and Nb_3Si. The Nb_3Si blocks did not decompose.

4) After heat treatment, the Nb_{SS} dendrites became continuous gradually, and secondary dendrites arms became coarser. In the DS18 specimen, the Ti-rich microstructure disappeared so that the Nb_3Si tended to be the matrix, and the eutectic Nb_{SS} interconnected and were uniformly distributed in the Nb_3Si matrix.

References

[1] Bewlay, B. P., Jackson, M. R., Zhao, J. C., Subramanian, P. R., Mendiratta, M. G., Lewandowski, J. J., Ultrahigh-temperature Nb-Silicide-based composites, MRSBulletin, 28 (2003) (9):646–653.

[2] Bewlay, B. P., Jackson, M. R., Zhao, J. C., Subramanian, P. R., A review of very-high temperature Nb-Silicide-based composites, Metall. Mater. Trans. A, 34 (2003):2043–52.

[3] Bewlay, B. P., Jackson, M. R., Zhao, J. C., Subramanian, P. R., Processinghigh-temperature refractory-metal Silicide in-situ composites, JOM, 51 (1999):32.

[4] Jackson, M. R., Bewlay, B. P., Rowe, R. G., Skelly, D. W., Lipsitt, H. A., high-temperature refractory metal-intermetallic composites, JOM, 48 (1996):39.

[5] Yao, C., Guo, X., Guo, H., Microstructural Characteristics of Intergrally Directionally Solidified Nb-Ti-Si based Ultrahigh Temperature Alloy with Crucibles, Acta Metallurgica Sinica, 44 (2008) (5):579.

[6] He, Y., Guo, X., Guo, H., Sun, Z., Microstructure and solid/liquid interface morphology evolution of integrally directionally solidified Nb-Silicide-based ultrahigh temperature alloy, Acta Metallurgica Sinica (EnglLett), 45 (2009):1035–1041.

[7] Yao, C., Guo, X., Preparation techniques and directionally solidified microstructure of niobium-based ultrahigh temperature alloys, Mater. Rev., 21 (2007) (12):65–68.

[8] Qu, S., Wang, R., Han, Y., Recent Progress in Research Oil Nb-Si System, Intermetallic. Mater. Rev., 16 (2002) (4):31–34.

[9] Wang, Y., Guo, X., Effect of solidifying rate on integrally directionally solidified microstructure and solid/liquid interface morphology of an Nb-Ti-Si based alloy, Acta Metallurgica Sinica (EnglLett) 46 (2010) (4):507.

[10] Zhou, Y., Hu, Z., Jie, W., Solidification Technology, Beijing: Mechanical Industry Press, 206, 1998.

[11] Ma, L., Yuan, S., Cui, R., Tang, X., Li, Y., Gao, M., Zhang, H., Interactions between Nb-silicide based alloy and yttria-mould during directional solidification, Int. Journal of Refractory Metals and Hard Materials, 30 (2012):96–101.

[12] Li, X., Chen, H., Sha, J., Zhang, H., The effects of melting technologies on the microstructures and properties of Nb-16Si-22Ti-2Al-2Hf-17Cr alloy, Materials Science and Engineering A, 527 (2010):6140–6152.

[13] Kang, Y., Qu, S. Song, J., Han, Y., Effect of directional solidification rate on microstructures and properties of Nb-Si system in situ composites, Acta Metallurgica Sinica, 44 (2008) (5):593.

[14] Jia, L., Guo, X., Yi, L., Effects of heat treatments on the microstructure of Nb-Si-based in-situ composites, Rare Metal Materials and Engineering, 37 (2008) (5):879–881.

[15] Li, Y., Miura, S., Ohsasa, K., Ma, C., Zhang, H., Ultrahigh-temperature Nbss/Nb5Si3 fully-lamellar microstructure developed by directional solidification in OFZ furnace, Intermetallics, 19 (2011):460–469.

[16] Guo, X., Gao, L., Microstructure and mechanical properties of nb based ultra high temperature alloy directionally solidified by EBFZM, Journal of Aeronautical Materals, 26 (2006) (3):47.

[17] Bewlay, B. P., Lipsitt, H. A., Jackson, M. R., Suliff, J. A., Investigation of high-temperature eutectic-based microcompsites, General Electric Company, Corporate Researchand Development Center, 1996.

[18] Xiao, Z., Zheng, L., Wang, L., Yang, L., Zhang, H., Microstructure evolution of Ti-47Al-2Cr-2Nb alloy in the liquid-metal-cooling (LMC) directional-solidification process, Journal of Wuhan University of Technology – Mater. Sci. Ed., 26 (2011) (2):197–201.